



HAL
open science

Methanol fuel processor and PEM fuel cell modeling for mobile application

Daniela Chrenko, Fei Gao, Benjamin Blunier, David Bouquain, Abdellatif Miraoui

► **To cite this version:**

Daniela Chrenko, Fei Gao, Benjamin Blunier, David Bouquain, Abdellatif Miraoui. Methanol fuel processor and PEM fuel cell modeling for mobile application. *International Journal of Hydrogen Energy*, 2010, 35 (13), pp.6863-6871. 10.1016/j.ijhydene.2010.04.022 . hal-02615343

HAL Id: hal-02615343

<https://hal.science/hal-02615343>

Submitted on 28 Jun 2024

HAL is a multi-disciplinary open access archive for the deposit and dissemination of scientific research documents, whether they are published or not. The documents may come from teaching and research institutions in France or abroad, or from public or private research centers.

L'archive ouverte pluridisciplinaire **HAL**, est destinée au dépôt et à la diffusion de documents scientifiques de niveau recherche, publiés ou non, émanant des établissements d'enseignement et de recherche français ou étrangers, des laboratoires publics ou privés.



Distributed under a Creative Commons Attribution - NonCommercial 4.0 International License

Methanol fuel processor and PEM fuel cell modeling for mobile application

Daniela Chrenko ^{a,*}, Fei Gao ^b, Benjamin Blunier ^b, David Bouquain ^b, Abdellatif Miraoui ^b

^a ISAT, University of Burgundy, Rue Mlle Bourgoise, 58000 Nevers, France

^b Transport and Systems Laboratory (SeT) - EA 3317/UTBM, Fuel cell Laboratory (FCLAB), University of Technology of Belfort-Montbéliard, Rue Thierry Mieg 90010, Belfort Cedex, France

The use of hydrocarbon fed fuel cell systems including a fuel processor can be an entry market for this emerging technology avoiding the problem of hydrogen infrastructure. This article presents a 1 kW low temperature PEM fuel cell system with fuel processor, the system is fueled by a mixture of methanol and water that is converted into hydrogen rich gas using a steam reformer. A complete system model including a fluidic fuel processor model containing evaporation, steam reformer, hydrogen filter, combustion, as well as a multi-domain fuel cell model is introduced. Experiments are performed with an IDATECH FCS1200™ fuel cell system. The results of modeling and experimentation show good results, namely with regard to fuel cell current and voltage as well as hydrogen production and pressure. The system is auto sufficient and shows an efficiency of 25.12%. The presented work is a step towards a complete system model, needed to develop a well adapted system control assuring optimized system efficiency.

1. Introduction

During the last years, low temperature fuel cell systems have shown improvements with regard to life time and reliability and they are getting closer to industrialization. However, fuel cell systems have in general to be supplied with hydrogen. Hydrogen is an energy carrier and has to be produced from other energy sources. As well conventional energy sources like hydrocarbons (oil, coal) as renewable energy sources, in form of electric energy or biofuels, can be used.

For the moment the existing hydrogen infrastructure is limited to some field test areas. In order to use the fuel cell technology without the need of a hydrogen infrastructure an on-board hydrogen production using a fuel processor can be

used. This article presents a combined fuel processor and fuel cell model in order to evaluate the feasibility of on-board hydrogen production for mobile application.

In this article a low temperature fuel cell system with integrated fuel processor unit is introduced. The described system is fueled with a mixture of methanol and water. A combined fuel processor and a fuel cell model are introduced. The goal of the model is that it can be used later as the base of a control structure development.

There are several fuel processor models available in the literature [1–4]. The existing fuel processor models can be distinguished by the fuel that is processed inside the system like diesel [5,6], gasoline [7] or methane/methanol [4,8–11]. The core of a fuel processor is the reformer. Inside the

* Corresponding author. Tel.: +33 3 84 58 36 00; fax: +33 3 84 58 36 36.
E-mail address: daniela.chrenko@utbm.fr (D. Chrenko).

reformer a long chain hydrocarbon is converted into hydrogen, water, short chain hydrocarbons (CO, CO₂, CH₄) and other residuals. As low temperature fuel cell systems are sensitive to pollution by sulfur and carbon dioxide, additional stages to remove those pollutants have to be integrated into the fuel processor. The existing models can be distinguished according to the description of the reformer only or the entire fuel processing unit [10–12]. Furthermore, most of the authors focus on either modeling [13,14] or experimentation [4,10,12]. In the presented work a fluidic system model is compared to experimental results.

The presented fuel cell model is based on the work of Gao and Blunier [15–17] and uses a multiphysic dynamic one dimensional model of a proton exchange membrane fuel cell stack.

The presented fuel cell system has an electrical power output of maximum 1 kW and is therefore in the same power range as the fuel processor described in [10,12].

2. Model

2.1. Fuel processor

2.1.1. System description

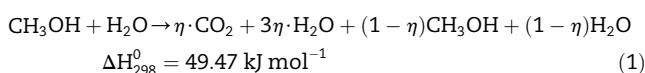
The main components of a fuel processor unit are (in the order they are flown through by the gas):

- evaporator;
- reformer;
- hydrogen filter;
- combustion.

The behavior of the different stages is presented in the following.

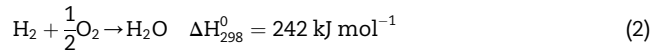
The IDATECH FCS1200™ fuel cell system is supplied by a mixture of methanol and water with 66 weight% of methanol and 34 weight% of deionized water. At normal conditions this mixture is liquid. As soon as the mixture gets into the fuel processor it is evaporated inside the *evaporation unit*. In order to evaporate the mixture, heat has to be supplied. During system heat up, the heat is supplied by an electrical resistance powered by the batteries. As soon as the fuel processor is in working conditions the heat is supplied by the combustion unit.

Then, the gaseous methanol-water-mixture enters into the second stage of the fuel processor, the so called *reformer unit*. Inside the fuel reformer the transformation from methanol and water into hydrogen and carbon dioxide takes place. This reaction is called steam reforming reaction as the hydrocarbon (methanol) is mixed with steam and no other gases are used. The steam reaction is endothermic; heat has to be supplied in order to keep the system at constant temperature. The steam reforming reaction containing a conversion efficiency factor is stated in (1). Actually, this catalytic reaction is not ideal; there are some side reaction leading to the formation of carbon monoxide and methane which are neglected in this case.



after the reforming the hydrogen rich gas mixture still contains residues of methanol and carbon monoxide that can be hazardous for the fuel cell stack. That is why the gas is separated from other components by means of a *hydrogen filter*. Only pure hydrogen can pass the filter. In order to have a high efficiency over the filter a big pressure difference or a long filtering time is needed. In this case, a robust and rapid hydrogen filter with a filtering efficiency of not more than 50% is used.

As well as the evaporation, the reforming stage needs a constant temperature to work in the desired condition. In order to keep a constant temperature, the not reformed methanol, reformation residues and the remaining hydrogen is mixed with air and combusted in the *combustion unit*. This combustion provides not only the heat needed to keep the fuel processor running, but also transforms the remaining hydrogen and carbon monoxide in non hazardous gases like water and carbon dioxide as introduced in (2) and (3).



the reforming and the combustion are separated from a fluidic point of view but coupled from a thermal point of view, the same approach has been presented by Simakov [11].

2.1.2. Modeling

The presented model takes into account the fluidic aspect of the fuel processor. The thermal aspect of the fuel processor is neglected. Hence, the heat production of the reactions are neglected and the reaction temperature inside each stage is fixed for the model. This assumption gives an idea about the fluidic behavior of the coupled system, without the need of time consuming non-linear temperature exchange calculations. It is furthermore assumed that the chemical reactions are rapid against the pressure dynamics, they are therefore assumed to be instantaneous for the fuel processor. The influence of the fuel processor volume on the pressure development is taken into account.

2.1.2.1. Fuel processor. The fuel processor is modeled using a limited number of elements. As there is no influence of the evaporation unit on the fluidic aspect of the gas it is not represented inside the model.

2.1.2.2. Reformer. The steam reforming reaction is modeled as an ideal reaction for the entire conversion of the methanol/water mixture as it is given in (1). The reaction is assumed to be instantaneous.

2.1.2.3. Filter. After the reforming reaction, the gas mixture is led through a hydrogen filter. Here the emphasis is put on a robust filter with a hydrogen filtering efficiency of around 50%. Different hydrogen-permeable and hydrogen-selective materials can be used for hydrogen filters, including carbon, ceramics and metals, namely palladium-alloys [18]. Inside the filter element, two main parameters are calculated: the pressure at the filter inlet and the gas composition. The gas

composition and pressure at the filter inlet is defined by the in- and outflowing quantity of gases in different compositions.

The description of the filter is based on the ideal gas law (4).

$$p = \frac{(\dot{n}_{in} + \dot{n}_{out} + \dot{n}_{H_2}) \cdot R \cdot T}{V} \quad (4)$$

with p the pressure before the filter in Pa, \dot{n}_{in} , \dot{n}_{out} and \dot{n}_{H_2} the molar gas flows entering the filter, exiting the filter and the hydrogen fed through the filter all in (mol s^{-1}) respectively, R the ideal gas constant ($8.31 \text{ J K}^{-1} \text{ mol}^{-1}$), T the temperature (K) and V the free volume of the fuel processor before the filter (m^3).

The quantity of pure hydrogen that is led through the filter depends on the pressure difference over the filter and can be described using an empiric linear nozzle description for laminar flows [19], equation (5).

$$q = k_{f-H_2} \cdot (p_{in} - p_{out}) \quad (5)$$

with k_{f-H_2} an empiric parameter ($\text{mol s}^{-1} \text{ Pa}^{-1}$). Inside the IDATECH FCS1200™ fuel cell system, less than 50% of the hydrogen passes through the filter. The remaining gases stays inside the diluted gas [18].

2.1.2.4. Connector to the fuel cell. The flow of pure hydrogen through the filter can be calculated knowing the pressure downstream of the filter.

The hydrogen pressure at the interface between the fuel processor and the fuel cell is calculated according to the inflowing and outflowing hydrogen and the free volume based on the ideal gas law as presented in (4).

In this case the hydrogen pressure at the fuel cell inlet has to be given by the fuel processor model; the hydrogen consumption is imposed by the fuel cell model.

2.1.2.5. Combustion and exhaust. The diluted gas exits the filter. It can be supposed that also the diluted gas has to overcome a flow resistance or throttle before entering the combustion chamber. Hence, the empiric linear nozzle description for laminar flows is used with a different empiric resistance parameter k_{f-res} to describe the flow of diluted gas passing from the filter into the combustion unit Fig. 2. As in the combustion unit the combustion gas is mixed with air, it can be assumed that the pressure in the combustion chamber is close to ambient pressure.

Inside the combustion chamber the combustion gas, still containing a considerable amount of hydrogen and some residues of methanol and carbon monoxide, is oxidized. The combustion heat is used for the evaporation and to maintain the steam reforming reaction. But as this connection is purely thermal and only fluidic aspects are considered in this case, the combustion is not modeled.

2.2. Multi-physic fuel cell stack model

A 1D multi-physical dynamic PEM fuel cell stack model that covers 3 major physical domains: electrical, fluidic and thermal is presented in this section. The fuel cell stack model is built from stacking the individual cell model together. Each cell is stacked one after another. The physical conditions of the cell N are calculated from cell $N-1$ and cell $N+1$.

2.2.1. Electrochemical cell model

The single cell voltage output can be expressed as follows:

$$V_{cell} = E - V_{act} - V_{ohm} \quad (6)$$

where E is the electromotive force (V), V_{act} the cell activation losses (V) and V_{ohm} the cell ohmic losses (V).

In the equation (6), it has to be noted that there is no concentration loss term. The gas pressures P_{O_2} and P_{H_2} used in equation (7) are the pressures at the interface of catalyst layer, the gas transport limits in the gas diffusion layers (GDLs) have been considered in the fluidic model hereafter. Thus, a concentration loss term is not needed in the equation (6).

The cell electromotive force is obtained from the Nernst equation:

$$E = 1.229 - 0.85 \cdot 10^{-3} (T - 298.15) + \frac{R \cdot T}{2F} \ln(\sqrt{P_{O_2}} \cdot P_{H_2}) \quad (7)$$

where T is the temperature of the layer (K), P_{O_2} the oxygen pressure (atm) at the interface of cathode catalyst layer, P_{H_2} the hydrogen pressure (atm) at the interface of anode catalyst layer, R the ideal gas constant ($8.31 \text{ J mol}^{-1} \text{ K}^{-1}$) and F the Faraday constant (96485 C mol^{-1}).

The cell activation losses can be expressed from the Tafel equation (derivate from Butler–Volmer equation):

$$V_{act} = \frac{R \cdot T}{\alpha \cdot n \cdot F} \ln\left(\frac{i}{j_0 \cdot S}\right) \quad (8)$$

where i is stack current (A), S the catalyze layer section area (m^2), n the number of electrons involved in the reaction, α the symmetry factor and j_0 the exchange current density (A m^{-2}).

The cell ohmic losses are mainly due to the membrane resistance. This loss can be obtained with membrane resistance expression after Joule's law:

$$V_{ohm} = R_{mem} \cdot i = \frac{i}{S} \int_0^\delta r(T, \lambda(z)) dz \quad (9)$$

with the expression of membrane resistivity:

$$r = \begin{cases} \frac{e^{[1268 \cdot (\frac{1}{T} - \frac{1}{303})]}}{0.1933} & \text{if } 0 < \lambda(z) \leq 1 \\ \frac{e^{[1268 \cdot (\frac{1}{T} - \frac{1}{303})]}}{0.5193 \cdot \lambda(z) - 0.326} & \text{if } \lambda(z) > 1 \end{cases} \quad (10)$$

where $\lambda(z)$ is the membrane local water content and δ its thickness (m), [20].

2.2.2. Cell fluidic model

The gas pressure drop in the channels due to the mechanical losses can be expressed by the Darcy–Weisbach Equation:

$$\Delta P = f_{darcy} \frac{\rho_{CV} \cdot L}{2D_{hydro}} V_s^2 \quad (11)$$

where f_{darcy} is the Darcy friction factor, D_{hydro} is the hydraulic diameter of the channels (m), V_s is the mean fluid velocity in the channels (m s^{-1}) and L is the length of the channel (m).

The phenomenon of the gas diffusion of each species i in the gas diffusion layers (GDL) is described by the Stefan–Maxwell equation:

$$\Delta P_i = \frac{\delta \cdot R \cdot T}{P_{tot} \cdot S} \sum_{j \neq i} \frac{P_i \cdot \frac{q_j}{M_j} - P_j \cdot \frac{q_i}{M_i}}{D_{ij}} \quad (12)$$

where δ is the GDL thickness (m), S is the GDL layer section (m^2), P_{tot} is the mean gas total pressure (Pa) in the GDL layer, M is the gas molar mass (kg mol^{-1}), j stands for species other than species i , and D_{ij} is the binary diffusion coefficient between the species i and j ($\text{m}^2 \text{s}^{-1}$).

The water balance in the membrane layer can be described by two different phenomenons: The electro-osmosis phenomenon in (13), and the back diffusion phenomenon in (14).

$$J_{\text{drag}} = \frac{n_{\text{sat}} \cdot \lambda(z)}{11} \cdot \frac{i}{2F} \cdot M_{\text{H}_2\text{O}} \quad (13)$$

$$J_{\text{back_diff}} = -\frac{\rho_{\text{dry}}}{M_n} \cdot D_\lambda \cdot \frac{d\lambda(z)}{dz} \cdot S \cdot M_{\text{H}_2\text{O}} \quad (14)$$

where $n_{\text{sat}} = 22$ is the electro-osmotic drag coefficient for maximum hydration condition, ρ_{dry} is the dry density of the membrane (kg m^{-3}), D_λ the mean water diffusion coefficient in the membrane ($\text{m}^2 \text{s}$), and M_n the equivalent mass of the membrane (kg mol^{-1}).

The total water mass flow (kg s^{-1}) in membrane can be then expressed:

$$q_{\text{H}_2\text{O,net}} = J_{\text{drag}} + J_{\text{back_diff}} \quad (15)$$

this equation is a differential equation of $\lambda(z)$ derivate by z (the membrane z -axis). By giving the boundary conditions for λ , the equation can be solved.

2.2.3. Cell thermal model

The thermal dynamic response of fuel cell is due to the thermal capacity of each cell layer. These temperature dynamics in each layer can be generally described as:

$$(\rho \cdot V \cdot C_p) \frac{dT}{dt} = \underbrace{Q_{\text{cond}}}_{\text{conduction}} + \underbrace{Q_{\text{forced_conv}}}_{\text{forced convection}} + \underbrace{Q_{\text{nat_conv}}}_{\text{natural convection}} + \underbrace{Q_{\text{mass}}}_{\text{convective mass flow}} + \underbrace{Q_{\text{internal_heats}}}_{\text{internal heat sources}} \quad (16)$$

where ρ is the mean layer density (kg m^{-3}), V is the layer volume (m^3), C_p is the layer thermal capacity ($\text{J kg}^{-1} \text{K}^{-1}$) and Q stands for the different types of heat flows entering or leaving the layer: conduction, forced convection, natural convection, radiation, convective mass flow and internal heating sources (J s^{-1}).

The heat flows due to conduction can be expressed according to Fourier's Law

$$Q_{\text{cond}} = \frac{2 \cdot \lambda_{\text{CV}} \cdot S_{\text{Section,CV}}}{\delta_{\text{CV}}} (T_{\text{boundary}} - T_{\text{CV}}) \quad (17)$$

where λ_{CV} is the thermal conductivity ($\text{W m}^{-1} \text{K}^{-1}$), $S_{\text{Section,CV}}$ the section of the fuel cell (m^2), T_{boundary} the cell boundary temperature (K), and δ_{CV} the cell thickness (m).

The heat flow due to forced convection in the fluid channels or natural convection can be written in the form of Newton's cooling Law:

$$Q_{\text{forced_conv}} = h_{\text{forced}} \cdot S_{\text{Section,CV}} (T_{\text{boundary}} - T_{\text{CV}}) \quad (18)$$

where is the forced convection heat transfer coefficient ($\text{W m}^{-2} \text{K}^{-1}$).

$$Q_{\text{nat_conv}} = h_{\text{nat_conv}} \cdot S_{\text{ext}} (T_{\text{amb}} - T_{\text{CV}}) \quad (19)$$

where $h_{\text{nat_conv,radia}}$ is the natural convection heat transfer coefficient ($\text{W m}^{-2} \text{K}^{-1}$), the external surface of the cell (m^2), and the ambient temperature (K).

The heat flow due to the mass transfer entering or leaving the cell can be calculated by:

$$Q_{\text{mass}} = \left[\sum_{\text{specie}} (q_{\text{specie}} \cdot C_{p,\text{specie}}) \right] \quad (20)$$

At last, the internal heat sources can be divided in 2 parts.

For cathode catalyst layers, an internal heat source due to the variation in entropy during the electrochemical reaction and to the activation losses can be expressed as follows:

$$Q_{\text{internal_heat1}} = \underbrace{-i_{\text{stack}} \frac{T_{\text{cata}} \cdot \Delta S}{2F}}_{\text{Entropy changes part}} + \underbrace{i_{\text{stack}} \cdot V_{\text{act}}}_{\text{Activation losses part}} \quad (21)$$

where $\Delta S = -163.185$ is the entropy change ($\text{J mol}^{-1} \text{K}^{-1}$) during the electrochemical reaction.

For the membrane layer, a source of heat due to the Joule effect of the membrane resistance can be obtained according to Joule's Law:

$$Q_{\text{internal_heat2}} = i_{\text{stack}}^2 \cdot R_{\text{mem}} \quad (22)$$

2.3. Parameters

2.3.1. Fuel processor

The model of the fuel processor contains a number of parameters. The only two empirical parameters ($k_{f-\text{H}_2}$ and $k_{f-\text{res}}$) have been determined by an optimization of the non-linear fuel processor model.

The modeling parameters are presented in Table 1.

2.3.2. Fuel cell

The one dimensional multi-physical dynamic PEM fuel cell stack model is a complex multi-domain model, still the model is entirely analytic and all the parameters in the model have a clear physical meaning. A detailed evaluation of fuel cell model is given by Gao et al. [15–17].

Table 1 – Main aspects of power sources in hybrid architectures.

	Description	Symbol	Unit	Value
INPUT	H ₂ consumption	q_{H_2}	mol s^{-1}	
	Methanol/ Water Inflow	q_{fuel}	mol s^{-1}	
Temp.	Fuel Processor before filter	T_{FP}	K	473.15
	Fuel Cell Input	T_{FC}	K	313.15
Volume	Fuel Processor	V_{FP}	m^3	10^{-3}
	Hydrogen storage before Fuel Cell	V_{FC}	m^3	2×10^{-3}
Pressure	Fuel Cell Input (reference value)	P_{FC}	Pa	1.8×10^{-5}
	Combustion Chamber	P_{comb}	Pa	1.2×10^{-5}
	Empiric param.	Flow resistance	$k_{f-\text{H}_2}$	$\text{mol s}^{-1} \text{Pa}$
	Flow resistance residue	$k_{f-\text{res}}$	$\text{mol s}^{-1} \text{Pa}$	1.2×10^{-7}
OUTPUT	H ₂ pressure at fuel cell inlet	P_{H_2}	Pa	

3. System experimentation and modeling

The studied system is an IDATECH FCS1200™ fuel cell system. This is a portable low temperature fuel cell system with an integrated steam reforming unit. It is designed as stand alone power generator. The IDATECH FCS1200™ fuel cell system is rated to provide 1000 W of DC power at 48 V. The IDATECH FCS1200™ fuel cell system is the overall system that uses a Ballard NEXA™ fuel cell as well as the fuel processor unit containing fuel supply, evaporation unit, reformer and hydrogen filter. At the same time a battery which is used to provide the power needed to start the fuel processor and fuel cell system. It is furthermore used for peak power shaving that cannot be followed by the fuel processor/fuel cell system due to its high time constant.

The IDATECH FCS1200™ fuel cell system is installed in a box of dimensions 70 cm² × 79 cm² × 62 cm² and has a weight of about 100 kg.

A photo of the overall system can be seen in Fig. 1.

A schematic fluidic representation of the IDATECH FCS1200™ fuel cell system is given in Fig. 2.

A schematic electrical representation of the IDATECH FCS1200™ fuel cell system is given in Fig. 3.

In this article a focus is put on the fuel processor and the fuel cell system. The converter, the battery and the power management are not considered.

During the experimentation at the UTBM a current profile was demanded from the system using a programmable charge Fig. 4, (1). The system current and voltage was measured using a data acquisition system from National Instruments Fig. 4, (2). The data acquisition and current profile have been controlled via LabView with a frequency of 1 k Hz. Furthermore, the IDATECH FCS1200™ fuel cell system provides an integrated data acquisition providing the fuel consumption, the fraction of current demanded from the fuel cell and from the battery Fig. 4, (3). At the same time the fuel cell behavior is supervised using its integrated data acquisition program the

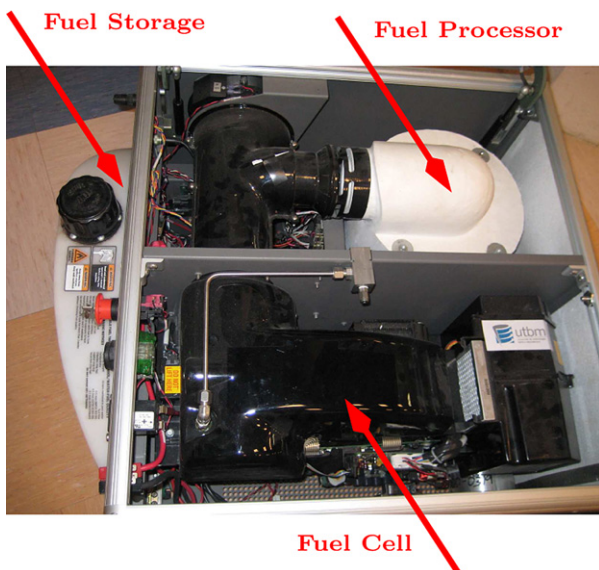


Fig. 1 – IDATECH FCS1200™ fuel cell system.

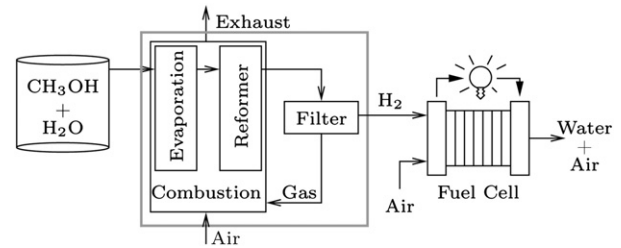


Fig. 2 – Fluidical scheme of the described fuel cell system.

NEXAMON Fig. 4, (4). This integrated data acquisition provides the fuel cell voltage, the hydrogen supply pressure, the mean fuel cell temperature and other values of interest.

The actual current demanded from the fuel cell, which was acquired during tests as well as the overall current demanded from the system are used as the two main input parameters for the fuel cell system simulation Fig. 4, (5). The system is modeled using MATLAB/Simulink software.

4. Modeling results and validation

Experiments are made using an IDATECH FCS1200™ fuel cell system. The experimental results are used to study the system and to validate the system model presented before.

4.1. Powers

The load that has to be supplied by the fuel cell system is defined by the current demanded from the charge. The presented power profile at the charge contains four steps of current of 5 A, representing power levels of 240 W, 480 W, 720 W and 960 W.

Fig. 5 shows, that the battery can either supply power (positive current values) or store power (negative current values).

The Ballard NEXA™ can only supply energy. Despite the remarkable changes in power demanded from the system, the fuel cell stack runs a relatively constant power level between 300 W and 700 W.

As the system is autonomous, the auxiliaries are supplied by the fuel cell stack. The main energy consumers are the fuel processor, with the fuel pump and the air pump for the residue combustion. Furthermore, the fuel cell stack has some auxiliary power consumption, mainly the system control and air fans [21]. Fig. 5 shows, that the auxiliary consumption is nearly constant and in the range of 110 W.

That is why the power at the converter is equal to the fuel cell power reduced by the auxiliary powers. The power at the

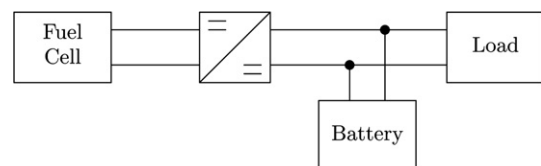


Fig. 3 – Electrical representation of the fuel cell system.

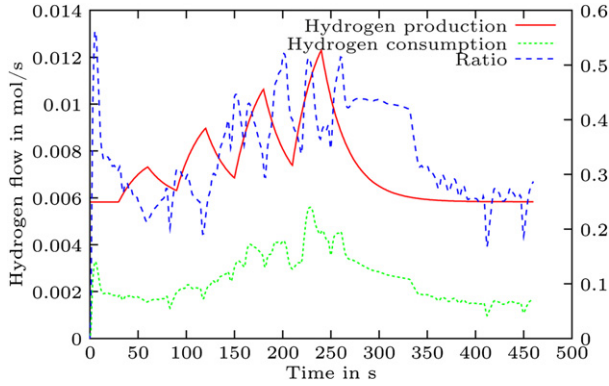


Fig. 7 – Comparison of available and consumed hydrogen flow.

combination of both results can be seen in Fig. 7. It is shown that the available amount of hydrogen is superior to the consumed hydrogen. The ratio between the both hydrogen flows shows an utilization factor between 20% and 50%. This value is in good accordance with the values of fuel ratio provided by IDATECH [18].

4.4. Hydrogen pressure

As it has been described in Section 2.1.2, the hydrogen pressure at the fuel cell inlet is defined by the empiric linearized nozzle equation for laminar flows, equation (5). This equation contains two empirical flow resistance constants (k_{f-H_2} and k_{f-res}). Those constants have been defined empirically using the observation that the hydrogen supply pressure is at the lower level of pressures accepted by the fuel cell system. Hence, the desired hydrogen pressure before the fuel cell system is known to be around 1.8 bar. The empirical parameters k_{f-H_2} and k_{f-res} are identified using a non-linear minimization of the error between the calculated and desired hydrogen pressure at the fuel cell inlet. The identified parameters are given in Table 1. The simulated hydrogen pressure depends on the hydrogen consumption of the fuel cell and the hydrogen production of the fuel processor both having a time constant when the system load is changing.

The desired pressure at the fuel cell input is fixed, the modeled hydrogen pressure at the fuel cell entrance is presented in Fig. 8. It shows that the hydrogen pressure at the fuel cell inlet is varying around 1.8 bar starting from an initial value of 1 bar. There are variations to higher pressures (up to 2.2 bar). The variations to higher pressures are not critical as the Ballard NEXA™ fuel cell system specification says that the system can accept inlet pressures up to 17 bar. It can also be seen that the pressure drop is limited to values of around 1.7 bar, this is the limit minimum of inlet pressure that has to be assured in order to keep the fuel cell running. It is thus shown in Fig. 8 that the modeling results are well adapted to the observations made during experimentation.

4.5. Stack voltage

It is also interesting to compare the modeled stack voltage with measured values. The modeling results are obtained by using

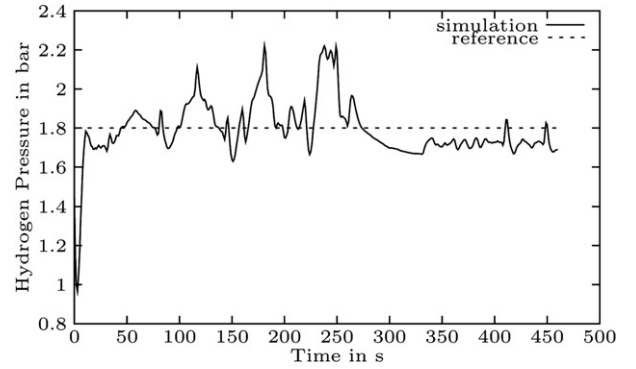


Fig. 8 – Modeled hydrogen pressure at the fuel cell entrance.

two input variables, the fuel cell current and the system current. The system current is the current delivered by the IDATECH FCS1200™ fuel cell system to the load. Only a part of the entire system current is delivered by the fuel cell. The rest is provided by the battery. The behavior of the battery is not described in this article. The current delivered by the fuel cell is also used to define the fuel flow to the fuel processor (see Section 4.2). The model of the fuel processor leads to a description of the hydrogen pressure at the fuel cell inlet. The measured fuel cell current has been used as input parameters of the fuel cell stack model. Finally, the hydrogen temperature at the fuel cell entrance has been fixed to a constant value of 313 K.

Using those three input parameters (hydrogen temperature, hydrogen pressure and fuel cell current) the fuel cell stack has been modeled according to the model introduced in Section 2.2. A comparison between the modeled and measured fuel cell stack voltage is presented in Fig. 9. It can be seen, that the modeled and measured voltage are in good accordance, some slight differences of maximum 0.8 V can be seen throughout the tests. Those differences can be described by the fact, that the modeled hydrogen pressure might differ from the real hydrogen pressure and that the real hydrogen temperature is not constant at the fixed value used for the model.

4.6. System efficiency

The calculation of the time dependent system efficiency is fastidious because the fuel consumption is, due to the hybridization with a battery, not proportional to the energy supplied.

As the focus of this work was put on the combination of methanol fuel processor and fuel cell system, the system efficiency over those two elements taking into account the auxiliary powers presented in Section 4.1 is studied here. Still, there is a time delay between the moment the fuel is supplied to the system and the moment the fuel is converted into electrical energy leading to considerable variations in the efficiency.

The efficiency is defined by (24):

$$\eta = \frac{\text{electrical energy supplied}}{\text{fuel flow} \times \text{enthalpy of overall reaction}} \quad (24)$$

$$\eta = \frac{U_{FC} \cdot I_{FC}}{q_{fuel} \cdot \Delta H_{298}^0}$$

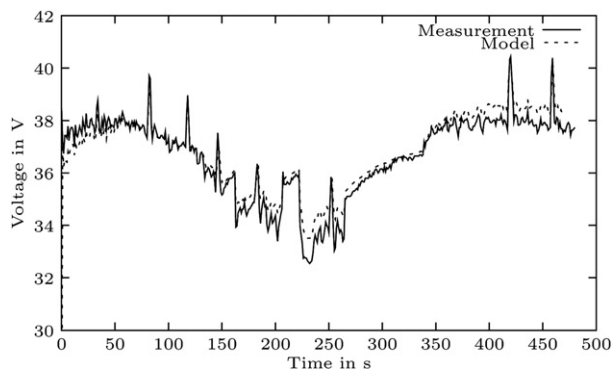


Fig. 9 – Comparison of measured and modeled fuel cell stack voltage.

the reaction enthalpy of the overall reaction is 385 kJ mol^{-1} , taking into account a production of gaseous water during steam reforming and liquid water inside the fuel cell.

In order to obtain a reliable system efficiency, the integral efficiency presented in (25) is regarded.

$$\eta = \frac{\int (U_{FC} \cdot I_{FC}) dt}{\int (q_{\text{fuel}} \cdot \Delta H_{298}^0) dt} \quad (25)$$

this leads to an overall system efficiency of 25.12%. Even if this results seem rather optimistic, they are in accordance with results presented for other systems of the same type [22,1].

As a matter of fact the system efficiency of a system including a methanol fuel processor and a fuel cell system is bound to be limited. Two conversion processes have to be effectuated, firstly during hydrogen production and secondly inside the fuel cell, each conversion imposes losses. With regard to the fuel cell efficiency improvements have to be made with regard to system efficiency and feasibility as has been described by Gao et al. [15]. The fuel processing unit is not yet as elaborated as the fuel cell and might offer some more room for improvement. Nevertheless, the fuel processing shows already the feature that the heat needed for evaporation and reforming is provided by burning the residues, thus optimizing the process. In any case, the production of hydrogen imposes some losses. Those losses are much more visible when they occur inside the vehicle compared to a decoupled hydrogen production [23].

5. Conclusion and perspectives

This article presents the combined system model of a methanol fuel processor and low temperature fuel cell system. The model is validated against experimental results from a IDA-TECH FCS1200™ fuel cell system. The fuel, a mixture of methanol and water, is transformed into a hydrogen rich gas inside the fuel processor consisting of four stages (evaporation, steam reformer, hydrogen filter, combustion). The fluidic model is leading to a description of the molar flows inside the fuel processor. The fuel cell system model is parametrized by the fuel processor model. It is presented by a one dimensional multi-physical dynamic PEM fuel cell stack model.

The system model is validated against experimental results with regard to fuel cell current and voltage, as well as hydrogen production and hydrogen pressure, all showing good accordance, with an overall system efficiency of 25.12%. Based on the observation the mode of fuel supply and the functioning of the hydrogen filter including the connected pressure development are discussed. The relatively high system efficiency can be partly explained by the fact that the fuel cell system stays in a constant and well adapted power range with slow dynamics, leading to the fact that it is used in its optimal efficiency range as well as the fact that the combustion of residue gases provides the thermal balance.

In the future, it is interesting to describe the thermal aspect of the fuel processor model, in order to refine the control the thermal aspect of the system. Furthermore, it is interesting to describe the entire hybrid system including the battery. This will lead to the development of the system control and the connection between the current demanded from the overall system in order to improve the system efficiency.

REFERENCES

- [1] Petterson LJ, Westerholm R. State of the art of multi-fuel reformers for fuel cell vehicles: problem identification and research needs. *International Journal of Hydrogen Energy* 2001;26:243–64.
- [2] Amphlett J, Mann RF, Peppley BA, Roberge PR, Rodrigues A, Salvador J. Simulation of a 250 kw diesel fuel processor/pem fuel cell system. *Journal of Power Sources* 1999;91:179–84.
- [3] Bowers BB, Zhao JL, Ruffo M, Khan R, Dattatraya D, Dushman N, et al. Onboard fuel processor for pem fuel cell vehicles. *International Journal of Hydrogen Energy* 2007;32:1437–42.
- [4] Lee M-T, Werhahn M, Hwang DJ, Hotz N, Greif R, Poulikakos D, et al. Hydrogen production with a solar steam-methanol reformer and colloid nanocatalyst. *International Journal of Hydrogen Energy* 2010;35:118–26.
- [5] Mengel C, Konrad M, Wruck R, Lucka K, Köhne H. Diesel steam reforming for pem fuel cells. *Journal of Fuel Cell Science and Technology* May 2008;5(021005). 021 005–1–021 005–5.
- [6] Kraaij G, Specchia S, Bollito G, Murtri L, Wails D. Biodiesel fuel processor for apu applications. *International Journal of Hydrogen Energy*; 2008. p. available online since 25 September 2008.
- [7] Boehme TR, Onder CH, Guzzella L. Dynamic mode of an autothermal gasoline fuel processor. *International Journal of Hydrogen Energy* 2008;33:6150–64.
- [8] Zahedi M, Rowshanzamira S, Eikanic M. Autothermal reforming of methane to synthesis gas: modeling and simulation. *International Journal of Hydrogen Energy*; 2009: 1–9.
- [9] Emonts B, Hansen JB, Joergensen SL, Höhlein B, Peters R. Compact methanol reformer test for fuel-cell power light-duty vehicles. *Journal of Power Sources* 1998;71:288–93.
- [10] Mathiak J, Heinzl A, Roes J, Kalk T, Kraus H, Brandt H. Coupling of a 2.5 kw steam reformer with a 1 kwel pem fuel cell. *Journal of Power Sources* 2004;131:112–9.
- [11] Simakov DSA, Sheituch M. Demonstration of a scaled-down autothermal membrane methane reformer for hydrogen generation. *International Journal of Hydrogen Energy* 2009; 34:8866–76.

- [12] Han J, Kim I-s, Choi K-S. Purifier-integrated methanol reformer for fuel cell vehicles. *Journal of Power Sources* 2000; 86:223–7.
- [13] Patel KS, Sunol AK. Dynamic behaviour of methane heat exchange reformer for residential fuel cell power generation system. *Journal of Power Sources* 2006;161: 503–12.
- [14] Chrenko D, Lecoq S, Herail E, Hissel D, Péra M-C. Static and dynamic modeling of a diesel fed fuel cell power supply. *International Journal of Hydrogen Energy* 2009;35: 1377–89.
- [15] Gao F, Blunier B, Miraoui A, El-Moudni A. Cell layer level generalized dynamic modelling of pemfc stack using vhdl-ams language. *International Journal of Hydrogen Energy* July 2009;34(13):5498–521.
- [16] Gao F, Blunier B, Miraoui A. A multiphysic dynamic 1d model of a proton exchange membrane fuel cell stack for real time simulation. *IEEE Transactions on Industrial Electronics*; 2009;. doi:10.1109/TIE.2009.2021177.
- [17] Blunier B, Miraoui A. Modelling of fuel cells using multi-domain vhdl-ams language. *Journal of Power Sources* 2007; 177(2):434–50.
- [18] Edlund D.J. Steam reformer with internal hydrogen purification. Redmond, OR; October 1999, 08/741,057.
- [19] Pukrushpan J.T. *Control of fuel cell power systems*, Springer, Ed. Springer; 2004.
- [20] Springer TE, Zawodzinski TA, Gottesfeld S. Polymer electrolyte fuel cell model. *Journal of Electrochemical Society* August 1991;138(8):2334–42.
- [21] Chrenko D, Péra M-C, Hissel D, Geweke M. Macroscopic modeling of a pemfc system based on equivalent circuits of fuel and oxidant supply. *ASME Journal of Fuel Cell Science and Technology* 2008;5. 011 015–1–011 015–5.
- [22] Aguirre PA, Mato RO, Mussati MC, Francesconi JA. Analysis of the energy efficiency of an integrated ethanol processor for pem fuel cell systems. *Journal of Power Sources* 2007;167:151–61.
- [23] Blunier B, Miraoui A. *20 Questions sur la Pile à Combustible*. Édition Technip, ISBN 978-2-7108-0928-9; 2009 [in french].